Plug Flow Reactor Model to Analyse Operating Conditions on the Dilute H_2SO_4-acid Hydrolysis of Sugarcane Bagasse at High-Solids Loading

Laura Plazas Tovar*, Maria Regina Wolf Maciel, Rubens Maciel Filho

University of Campinas, UNICAMP, Zipcode 13083–852, Campinas–SP, Brazil
lplazast@feq.unicamp.br

Previous kinetic modelling for dilute H_2SO_4-acid hydrolysis of sugarcane bagasse operated using batch reactor led to conclude that hemicellulose conversion, about 75 % of theoretical, was possible to be reached using 1.0 % w v^{-1} H_2SO_4 solution, solid load equal to 20 % and 80 min of operation. The present study aims to expand the fundamental understanding of the kinetic involved in this process. A continuous process isothermally performed in a plug flow reactor at dynamic was proposed and studied. H_2SO_4-acid hydrolysis of 200 kg h^{-1} of sugarcane bagasse using 1.0 % w v^{-1} H_2SO_4 solution, solid load equal to 20 %, 60 min and a reactor length of 1.30 m (with a cross-sectional area equal to 1 m^2) at 121 $^{\circ}$C resulted in yields of 59.70 % for xylose, 2.00 % for arabinose, 8.46 % for glucose, 8.42 % for acetic acid, 0.73 % for furfural, 0.12 % for 5-hydroxymethylfurfural and 0.00 % for levulinic acid which means more than 72 % of the hemicellulose (related to 30.99 % in the raw material) was easily hydrolyzed with similar inhibitors yields values when compared to process in batch configuration reported as: 8.43 % acetic acid, 0.96 % furfural, 0.16 % 5-hydroxymethylfurfural and 0.29 % levulinic acid. Hence, both reactors are equivalent in terms of the influence of the acid solution concentration and solids loading. However, plug flow reactor configuration reduces the time required to proceed with the H_2SO_4-acid hydrolysis.

1. Introduction

Nowadays, sugarcane bagasse is a target of various studies aimed at using its energy potential with respect to the production of mobility biofuel to substitute gasoline and attend the future demand for energy in the transport sector as: in Brazil for between 20 – 25 % (Tavares et al., 2011) and in the United States for between approximately 20 – 30 % (Krishnan et al., 2010); although its use is not restricted to this purpose. One of the primary challenges involving the lignocellulosic ethanol (in this work referenced as biofuel) production is the pre-treatment to remove the compositional and structural barriers of lignocellulosic materials, leading to an improvement in the percentage of hydrolysis and increasing yields of fermentable sugars (from cellulose and hemicellulose) efficient and economically viable. In this sense, acid hydrolysis of the several feedstock has been published in the open literature and used for obtaining glucose (Saeman, 1945), xylose (Lavarack et al., 2002), levulinic acid (Girisuta et al., 2007) and 5-hydroxymethylfurfural (Chang et al., 2006). Theoretical and experimental studies over the several feedstock have been performed in: (i) batch reactor to process: hardwood poplar (Kim et al., 2013), sugarcane bagasse (Tovar et al., 2013), wood sawdust (Islam et al., 2011) and sorghum straw (Herrera et al., 2004), and (ii) continuous reactors to process: sugarcane bagasse (Jaramillo et al., 2013; Lopez-Arenas and Sales-Cruz, 2012) and hardwood (Converse et al., 1989). Therefore, being justified the use of sugarcane bagasse to the production of biofuel, Tovar et al. (2013) and Lavarack et al. (2002) reported a full kinetic study (in batch reactor) showing the effects of solid-to-liquid ratio, acid solution concentration and reaction time on the sugars and inhibitors yields. The first authors showed that the glucose, 5-hydroxymethylfurfural and levulinic acid yields tend to increase along time as the acid solution concentration rises from 1.0 % to 3.0 % w v^{-1}. Moreover, a combination between high solid-to-liquid ratio and high acid solution concentration showed that xylose sugar decomposition rate increases reducing the

sugar yield. Similar results were obtained by Lavarack et al. (2002), concluding that decreasing the solid-to-liquid ratio reduced the rate at which the xylose decomposed. On the other hand, Jaramillo et al. (2013) proposed a deterministic model for a plug flow reactor taking into account the volume change of the reaction media during the hydrolysis process. Comparisons between batch and continuous reactors concluded that both reactors are mostly equivalent in terms of the influence of the solid-to-liquid ratio on xylose and glucose yields.

This study aims to expand the fundamental understanding of the kinetic involved in this process, since acid hydrolysis may be an important step of the second generation bioethanol production. A plug flow reactor (Figure 1) isothermally operated (at 121 °C) at dynamic behavior for dilute H_2SO_4-acid hydrolysis of sugarcane bagasse, to produce fermentable sugar (xylose yield from hydrolysis of hemicellulose) taking into account the influence of the solid-to-liquid ratio and the intraparticle diffusion of sulfuric acid into sugarcane bagasse, was proposed and studied .

2. Proposed kinetic model to acid hydrolysis in plug flow reactor

The model of the H_2SO_4-acid hydrolysis reactions of sugarcane bagasse in a PFR and the subsequent formation of by-products can be outlined in Figure 2. The balance equations were developed based on the following assumptions: (i) temperature and acid solution concentration are uniform along the reactor; (ii) effects of different particle size of sugarcane bagasse are neglected; (iii) there are not external mass transfer resistances to the solid; (iv) influences of internal mass transfer were considered by an intraparticle diffusion of sulfuric acid into sugarcane bagasse fibres reported in Kim and Lee (2002) (at 121 °C acid diffusivity equals De=5.5712x10^{-8} m^2 min^{-1}) (v) there are not radial and axial diffusion and (vi) the velocity profile across the radius is uniform.

Based on the mechanism displayed in Figure 2, the set of partial differential equations is presented in Table 1. The resulting system was solved using the method of lines (discretization of spatial (z domain) derivatives). Iterative computation process was implemented using the FORTRAN 90 language using the DLSODES subroutine. The FORTRAN code was compiled and executed by a Compaq® FORTRAN.
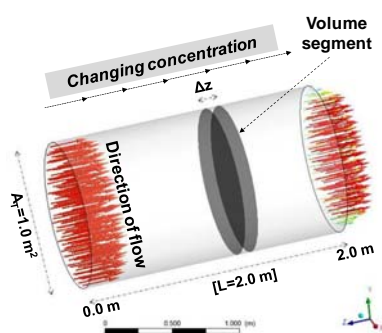

Figure 1: Schematic diagram of the plug flow reactor (PFR) to model and to simulate the H_2SO_4-acid hydrolysis of sugarcane bagasse
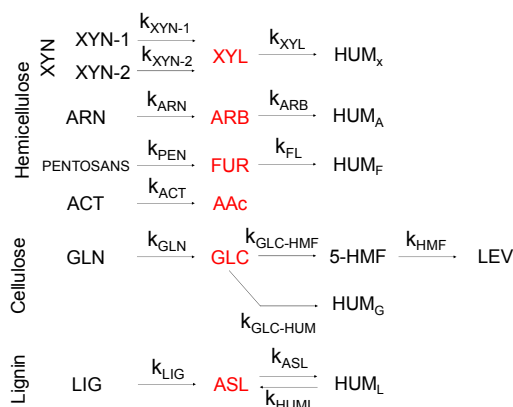
Figure 2: Kinetic mechanisms for the H_2SO_4-acid hydrolysis of sugarcane bagasse.

2.1 Boundary conditions and kinetic constants

Dirichlet conditions: At entrance of the PFR (Figure 1) was defined a set of values for concentrations of *[XLY], [ARB], [FUR], [AAc], [GLC], [5-HMF], [LEV]* and *[ASL]* equal to zero (g/100 g$_{sugarcane\_bagasse(SCB)}$). On the other hand, at the first point in z domain the concentrations of *[XYN-1], [XYN-2], [ARN], [Pentosans], [ACT], [GLN]*, and *[LIG]* correspond to the chemical composition of the raw material. It was determined by analytical two step acid hydrolysis followed by chromatographic analysis of the hydrolysate following the standard National Renewable Energy Laboratory protocols (NREL, 2013) (see Table 1).

Neumann condition: At the end point of discretization in z domain was fixed the value for the partial derivative with respect to z as zero ($[C_i]_N = [C_i]_{N-1}$).

Tables 2 and 3 present the data set and kinetic constants, respectively, used in the model and simulation of a PFR to analysis operating conditions on the dilute H_2SO_4-acid hydrolysis of sugarcane bagasse at high solid loading (20 %).

Table 1: Set of partial differential equations to model the H_2SO_4-acid hydrolysis reactions in a PFR

Reaction type	Partial differential equation	Boundary conditions	
		Dirichlet	Neumann
Xylose formation and degradation	$\dfrac{\partial[XYN-1]}{\partial t}=D_e\dfrac{\partial^2[XYN-1]}{\partial z^2}-\upsilon\dfrac{\partial[XYN-1]}{\partial z}-k_{XYN-1}[XYN-1]$ $\dfrac{\partial[XYN-2]}{\partial t}=D_e\dfrac{\partial^2[XYN-2]}{\partial z^2}-\upsilon\dfrac{\partial[XYN-2]}{\partial z}-k_{XYN-2}[XYN-2]$ $\dfrac{\partial[XYL]}{\partial t}=D_e\dfrac{\partial^2[XYL]}{\partial z^2}-\upsilon\dfrac{\partial[XYL]}{\partial z}+k_{XYN-1}[XYN-1]+k_{XYN-2}[XYN-2]-\phi k_{XYL}[XYL]$ $\dfrac{\partial[HUM_X]}{\partial t}=D_e\dfrac{\partial^2[HUM_X]}{\partial z^2}-\upsilon\dfrac{\partial[HUM_X]}{\partial z}+\phi k_{XYL}[HUM_X]$	$[XYN-1]|_1=16.13\,g/100g_{SCB}$ $[XYN-2]|_1=6.27\,g/100g_{SCB}$ $[XYL]|_1=0.00\,g/100g_{SCB}$ $[HUM_X]|_1=0.00\,g/100g_{SCB}$	$\left.\dfrac{\partial[C_i]}{\partial z}\right|_N=\dfrac{[C_i]|_N-[C_i]|_{N-1}}{\Delta z}$
Arabinose formation and degradation	$\dfrac{\partial[ARN]}{\partial t}=D_e\dfrac{\partial^2[ARN]}{\partial z^2}-\upsilon\dfrac{\partial[ARN]}{\partial z}-k_{ARN}[ARN]$ $\dfrac{\partial[ARB]}{\partial t}=D_e\dfrac{\partial^2[ARB]}{\partial z^2}-\upsilon\dfrac{\partial[ARB]}{\partial z}+k_{ARN}[ARN]-\phi k_{ARB}[ARB]$ $\dfrac{\partial[HUM_A]}{\partial t}=D_e\dfrac{\partial^2[HUM_A]}{\partial z^2}-\upsilon\dfrac{\partial[HUM_A]}{\partial z}+\phi k_{ARN}[ARB]$	$[ARN]|_1=1.88\,g/100g_{SCB}$ $[ARB]|_1=0.00\,g/100g_{SCB}$ $[HUM_A]|_1=0.00\,g/100g_{SCB}$	
Furfural formation and degradation	$\dfrac{\partial[Pentosans]}{\partial t}=D_e\dfrac{\partial^2[Pentosans]}{\partial z^2}-\upsilon\dfrac{\partial[Pentosans]}{\partial z}-k_{PEN}[Pentosans]$ $\dfrac{\partial[FUR]}{\partial t}=D_e\dfrac{\partial^2[FUR]}{\partial z^2}-\upsilon\dfrac{\partial[FUR]}{\partial z}+k_{PEN}[Pentosans]-\phi k_{FL}[FUR]$ $\dfrac{\partial[HUM_F]}{\partial t}=D_e\dfrac{\partial^2[HUM_F]}{\partial z^2}-\upsilon\dfrac{\partial[HUM_F]}{\partial z}+\phi k_{FL}[FUR]$	$[Pentosans]|_1=24.28\,g/100g_{SCB}$ $[FUR]|_1=0.00\,g/100g_{SCB}$ $[HUM_F]|_1=0.00\,g/100g_{SCB}$	
Acetic acid formation	$\dfrac{\partial[ACT]}{\partial t}=D_e\dfrac{\partial^2[ACT]}{\partial z^2}-\upsilon\dfrac{\partial[ACT]}{\partial z}-k_{ACT}[ACT]$ $\dfrac{\partial[AAc]}{\partial t}=D_e\dfrac{\partial^2[AAc]}{\partial z^2}-\upsilon\dfrac{\partial[AAc]}{\partial z}+k_{ACT}[ACT]$	$[ACT]|_1=3.63\,g/100g_{SCB}$ $[AAc]|_1=0.00\,g/100g_{SCB}$	
Glucose formation and degradation	$\dfrac{\partial[GLN]}{\partial t}=D_e\dfrac{\partial^2[GLN]}{\partial z^2}-\upsilon\dfrac{\partial[GLN]}{\partial z}-k_{GLN}[GLN]$ $\dfrac{\partial[GLC]}{\partial t}=D_e\dfrac{\partial^2[GLC]}{\partial z^2}-\upsilon\dfrac{\partial[GLC]}{\partial z}+k_{GLN}[GLN]-\phi(k_{GLC-HMF}+k_{GLC-HUM})[GLC]$ $\dfrac{\partial[5-HMF]}{\partial t}=D_e\dfrac{\partial^2[5-HMF]}{\partial z^2}-\upsilon\dfrac{\partial[5-HMF]}{\partial z}+\phi k_{GLC-HMF}[GLC]-\phi k_{HMF}[LEV]$ $\dfrac{\partial[LEV]}{\partial t}=D_e\dfrac{\partial^2[LEV]}{\partial z^2}-\upsilon\dfrac{\partial[LEV]}{\partial z}+\phi k_{HMF}[5-HMF]$ $\dfrac{\partial[HUM_G]}{\partial t}=D_e\dfrac{\partial^2[HUM_G]}{\partial z^2}-\upsilon\dfrac{\partial[HUM_G]}{\partial z}+\phi k_{GLC-HUM}[GLC]$	$[GLN]|_1=41.67\,g/100g_{SCB}$ $[GLC]|_1=0.00\,g/100g_{SCB}$ $[5-HMF]|_1=0.00\,g/100g_{SCB}$ $[LEV]|_1=0.00\,g/100g_{SCB}$ $[HUM_L]|_1=0.00\,g/100g_{SCB}$	
Acid soluble lignin formation	$\dfrac{\partial[LIG]}{\partial t}=D_e\dfrac{\partial^2[LIG]}{\partial z^2}-\upsilon\dfrac{\partial[LIG]}{\partial z}-k_{LIG}[LIG]$ $\dfrac{\partial[ASL]}{\partial t}=D_e\dfrac{\partial^2[ASL]}{\partial z^2}-\upsilon\dfrac{\partial[ASL]}{\partial z}+k_{LIG}[LIG]+\phi k_{HUML}[HUM]-\phi k_{ASL}[ASL]$ $\dfrac{\partial[HUM_L]}{\partial t}=D_e\dfrac{\partial^2[HUM_L]}{\partial z^2}-\upsilon\dfrac{\partial[HUM_L]}{\partial z}-\phi k_{HUML}[HUM_L]+\phi k_{ASL}[ASL]$	$[LIG]|_1=17.08\,g/100g_{SCB}$ $[ASL]|_1=0.00\,g/100g_{SCB}$ $[HUM_L]|_1=0.00\,g/100g_{SCB}$	

Table 2: Set of variable to model and simulate the H_2SO_4-acid hydrolysis reactions in a PFR

Variable	Unit	Value	Variable	Unit	Value
Liquid density, ρ_L	kg m^{-3}	1000	Liquid-to-solid ratio, ϕ_{LS}	-	5
Solid density, ρ_S	kg m^{-3}	1500	Initial feed mass flow of solid, m_{S0}	kg h^{-1}	200
Reaction temperature, T	C	121	Initial feed mass flow of liquid, $m_{L0}=\phi_{LS}\times m_{S0}$	kg h^{-1}	1000
Reaction time, t	min	100	Feed liquid volumetric flow, $\upsilon_{L0}=m_{L0}\times\rho_L$	m^3 h^{-1}	1
Acid concentration, A	%w v^{-1}	1.0	Reactor length, L	m	2
Solid loading, S	%	20	Cross-sectional area, A_T	m^2	1
Solid-to-liquid ratio, ϕ_{SL}	-	0.2	Flow velocity, υ	m min^{-1}	1/60

Table 3: Kinetic rates of sugar and inhibitors released for the H_2SO_4-acid hydrolysis (Tovar et al., 2013)

Kinetic rate	Unit	Value	Kinetic rate	Unit	Value	Kinetic rate	Unit	Value
k_{XYN-1}	min^{-1}	5.8494×10^{-2}	k_{PEN}	min^{-1}	1.1825×10^{-4}	k_{HMF}	min^{-1}	2.4482×10^{-1}
k_{XYN-2}	min^{-1}	3.9564×10^{-2}	k_{FL}	min^{-1}	6.4828×10^{-3}	$k_{GLC-HUM}$	min^{-1}	4.1235×10^{-6}
k_{XYL}	min^{-1}	1.6574×10^{-3}	k_{ACT}	min^{-1}	1.0239×10^{-1}	k_{LIG}	min^{-1}	5.1798×10^{-3}
k_{ARN}	min^{-1}	9.9924×10^{-2}	k_{GLN}	min^{-1}	1.6979×10^{-3}	k_{ASL}	min^{-1}	1.5709×10^{-1}
k_{ARB}	min^{-1}	9.1645×10^{-5}	$k_{GLC-HMF}$	min^{-1}	3.3283×10^{-3}	k_{HUML}	min^{-1}	3.2990×10^{-2}

3. Results and discussion

From the results obtained in Figure 3, it can be summarized that the hydrolysate mass yield rises mainly due to the recovery of hemicellulose. However, once the reaction time increases from 60 to 100 min and reactor length from 1.30 to 2.00 m, it is worthy to–note that the hydrolysate mass yield does not change aiming 29.0 % w w^{-1}. However, simulated data of acid hydrolysis in a PFR system were compared with experimental data obtained in batch configuration which reported a hydrolysate mass yield of 31.17 % w w^{-1}. Hence, both reactors configurations are basically equivalent in terms of the influence of the reaction time on hydrolysate mass yield.
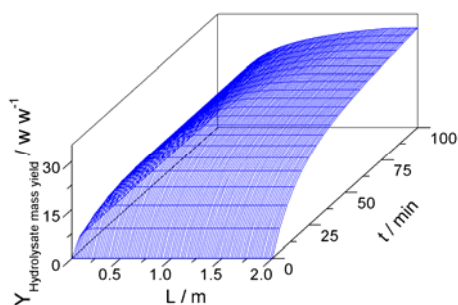

Figure 3: Profile of hydrolysate mass yield of sugarcane bagasse

Figures 4A – 4C exhibit the contour plot of the solubilized fraction estimated by simulation using a PFR configuration. Solubilized fraction or conversion corresponds to the evolution of hemicellulose removal and cellulose and lignin dissolution during reaction time (0 – 100 min) along the reactor length. It is noted that conversion of hemicellulose increases up to 1.30 m and 60 min, respectively. Under these conditions, 72 % of the total hemicellulose was removed. With regard to lignin, similar behavior is also exhibited when the reaction time is lifted from 0 to 80 min, and reactor length attained 1.30 m. However, lignin dissolution aimed 14 %. Nevertheless, once the reaction time and reactor length increases, it is worthy to observe that the relative content of cellulose in the hydrolysate rises. This reflects that cellulose is affected by the acid but also by the time and reactor length.

With further examination upon Figure 5A – 5G, it is evident that reaction time presents significant effect on the hemicellulose removal and consequently on the production of sugars (xylose, glucose and arabinose) as well as on the formation of by-products (furfural, 5-hydroxymethylfurfural, levulinic acid and acetic acid). Thus, xylose results from the hydrolysis of hemicellulose and the acid attack carries out to break xylose bonds down to furfural (degradation product). Similarly, glucose mainly from cellulose hydrolysis can decompose into 5-hydroxymethylfurfural. However, glucose and 5-hydroxymethylfurfural exhibited concentrations lower than those of xylose and furfural, respectively.

Recognizing the formation characteristics of sugars and inhibitors with increasing reaction time and reactor length it has been shown that selectivity percentage of furfural and levulinic acid grows with reaction time, that is, at 100 min, the higher the furfural and levulinic acid selectivity are: 1.03 % and 2.31 %, respectively (Figures 6A and 6C). Their selectivity values are somewhat lower than the batch reactor configuration study (1.27 % and 2.55 %, respectively); however, the case study of a batch reactor and plug flow reactor reported a similar value for 5-hydroxymethylfurfural selectivity (1.48 % and 1.50 %, respectively, Figure 6C).
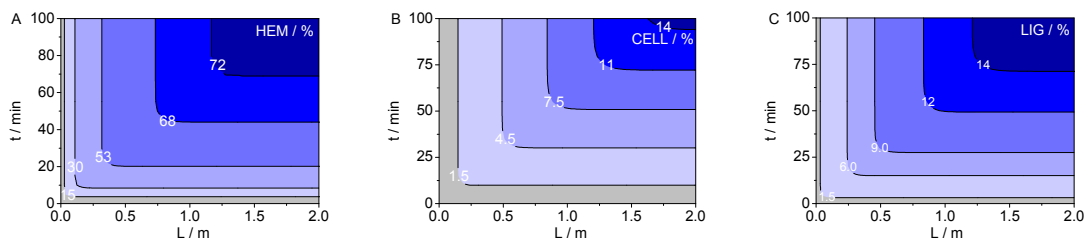

Figure 4: Distributions of conversions of: A. Hemicellulose (HEM), B. Cellulose (CELL) and C. Lignin (LIG)
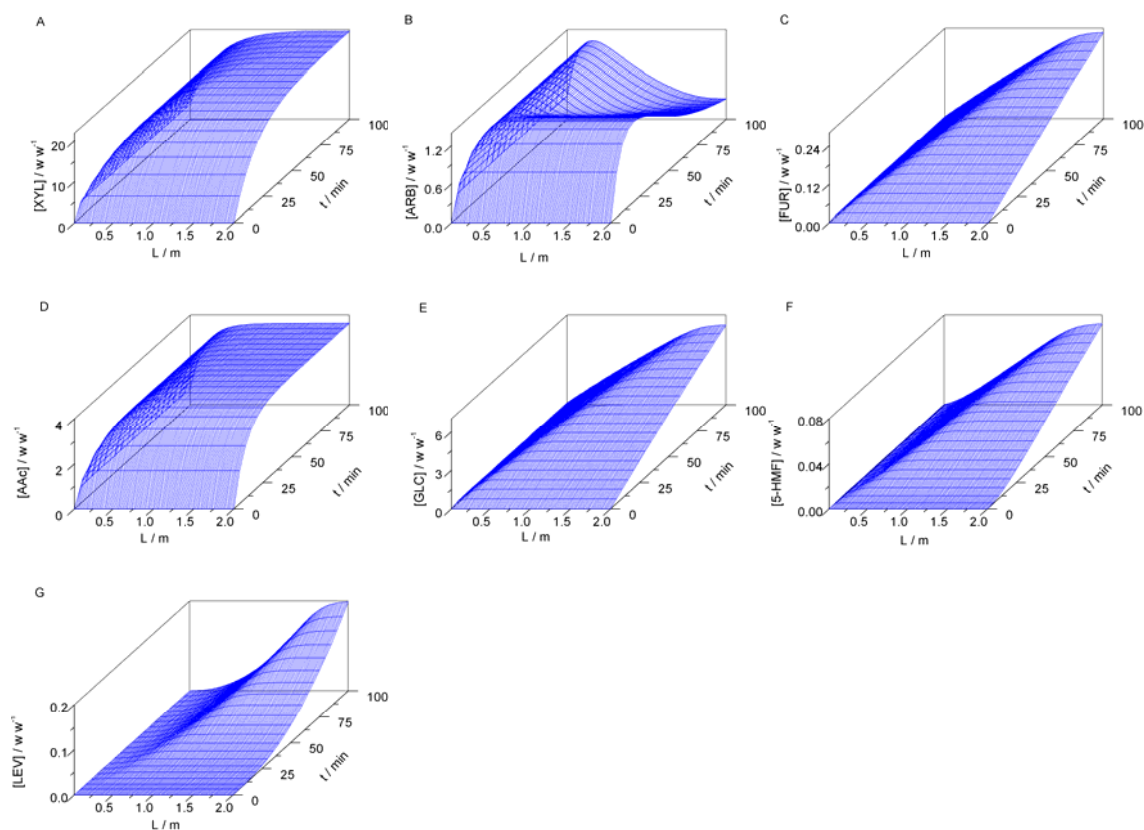
Figure 5: Distributions of concentrations of: A. Xylose ([XYL]), B. Arabinose ([ARB]), C. Furfural ([FUR]), D. Acetic acid ([AAc]), E. Glucose ([GLC]), F. 5-Hydroxymethylfurfural ([5-HMF]) and G. Levulinic acid ([LEV])

As it is shown in Figures 6A - 6C, once hydrolysis takes place the liquid phase increases while reducing the xylose concentration and increasing the furfural concentration. It is noted that does not exist minimum furfural selectivity. Alternatively, it is possible to control the 5-hydroxymethylfurfural selectivity along the PFR reactor (up to 1.30 m).
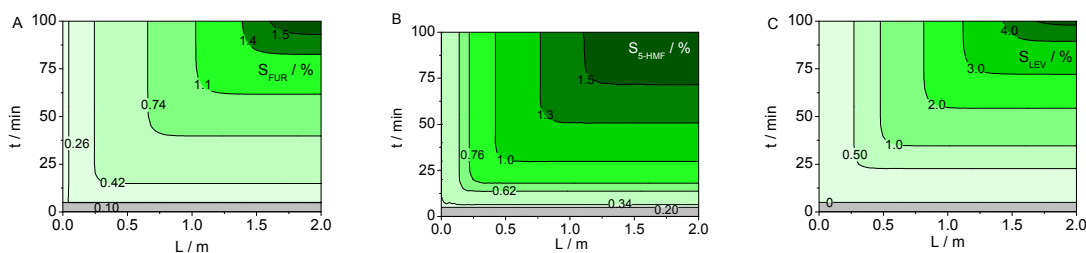

Figure 6: Distributions of inhibitors selectivity: A. Furfural (S_{FUR}), B. 5-hydroxymethylfurfural (S_{5-HMF}) and C. Levulinic acid (S_{LEV})

4. Conclusions

The PFR model to analyze the H_2SO_4-acid hydrolysis reactions of sugarcane bagasse comprised a system of partial differential equations describing temporal variations of material along the reactor length. This study incorporated, into the theoretical model, the intraparticle diffusion of sulfuric acid into sugarcane bagasse proposed by Kim and Lee (2002). Simulated results showed that both reactors (batch and plug flow reactors) are basically equivalent in terms of sugars concentration and hydrolysate mass yield. Therefore, using the proposed deterministic model for plug flow reactor, results give guidelines for improving the process efficiency related to reaction time. About 60 min, 1.0 % w v^{-1} H_2SO_4 acid solution

concentration, solid load equal to 20 %, 121 °C and 1.30 m of reactor length was enough to attain a yield of xylose of 59.70 %, which means that about 72 % of the hemicellulose is easily hydrolyzed. After xylose yields reach a maximum, further decomposition to furfural starts rapidly.

Nomenclature

k_{XYN-1} the rate of conversion of xylan easy-to-hydrolysis (*XYN-1*) to xylose (*XYL*); k_{XYN-2} is the rate of conversion of xylan hard-to-hydrolysis (*XYN-2*) to xylose (*XYL*); k_{XYL} is the rate of decomposition of xylose (*XYL*); k_{ARN} is the rate of conversion of arabinan (*ARN*) to arabinose (*ARB*); k_{ARB} is the rate of decomposition of arabinose (*ARB*) into decomposition products (*HUM$_A$*); k_{PEN} is the rate of conversion of pentosans to furfural (*FUR*); k_{FL} is the rate of decomposition of furfural (*FUR*) into decomposition products (*HUM$_P$*); k_{ACT} is the rate of conversion of acetyl groups linked to sugars (*ACT*) to acetic acid (*AAc*); k_{GLN} is the rate of conversion of glucan (*GLN*) to glucose (*GLC*); $k_{GLC-HMF}$ is the rate of decomposition of glucose (*GLC*) into 5-hydroxymethylfurfural (*5-HMF*); $k_{GLC-HUM}$ is the rate of decomposition of glucose (*GLC*) into decomposition products (*HUM$_G$*); k_{HMF} is the rate of decomposition of 5-hydroxymethylfurfural (*5-HMF*) into levulinic acid (*LEV*); k_{LIG} is the rate of conversion of lignin (*LIG*) to acid soluble lignin (*ASL*); k_{ASL} is the rate of decomposition of acid soluble lignin (*ASL*) into decomposition products (*HUM$_L$*); k_{HUML} is the rate of formation of acid soluble lignin with precursor decomposition products (HUM$_L$).

References

Chang C., Ma X., Cen P., 2006, Kinetics of levulinic acid formation from glucose decomposition at high temperature, Chinese J. Chem. Eng. 14, 708-712.

Converse A.O., Kwarteng I.K., Grethlein H.E., Ooshima H., 1989, Kinetics of thermochemical pretreatment of lignocellulosic materials, Appl. Biochem. Biotechnol., 20-21, 63-78.

Girisuta B., Janssen L.P.B.M., Heeres H.J., 2007, Kinetic study on the acid-catalyzed hydrolysis of cellulose to levulinic acid, Ind. Eng. Chem. Res., 46, 1696-1708.

Herrera A., Téllez-Luis S.J., González-Cabriles J.J., Ramírez J.A., Vázquez M., 2004, Effect of the hydrochloric acid concentration on the hydrolysis of sorghum straw at atmospheric pressure, J. Food Eng., 63, 103-109.

Islam S.M.R., Sakinah A. M. M., 2011, Kinetic modeling of the acid hydrolysis of wood sawdust, Int. J. Chem. Environ. Eng., 2, 333-337.

Jaramillo O.J., Gómez-García M.A., Fontalvo J., 2013, Prediction of acid hydrolysis of lignocellulosic materials in batch and plug flow reactors, Bioresour. Technol., 142, 570-578.

Kim Y., Kreke T., Ladisch M.R., 2013, Reaction mechanisms and kinetics of xylo-oligosaccharide hydrolysis by dicarboxylic acids, AIChE J., 59, 188-199.

Kim S.B., Lee Y.Y., 2002, Diffusion of sulfuric acid within lignocellulosic biomass particles and its impact on dilute-acid pretreatment, Bioresour. Technol., 83, 165-171.

Krishnan C., da Costa Sousa L., Jin M., Chang L., Dale B. E., Balan V., 2010, Alkali-based AFEX pretreatment for the conversion of sugarcane bagasse and cane leaf residues to ethanol, Biotechnol. Bioeng., 107, 441-450.

Lavarack B.P., Griffin G.J., Rodman D., 2002, The acid hydrolysis of sugarcane bagasse hemicellulose to produce xylose, arabinose, glucose and other products, Biomass Bioenergy, 23, 367–380.

López-Arenas T., Sales-Cruz M., 2012, Steady state analysis and optimization of a continuous reactor for acid pretreatment of lignocellulosic biomass, Chemical Engineering Transactions, 29, 1567-1572, DOI: 10.3303/CET1229262.

National Renewable Energy Laboratory (NREL), 2013. In Chemical Analysis and Testing Laboratory Analytical Procedures. 2013. <www.nrel.gov/biomass/analytical_procedures.html>, Accessed 11.01.2013.

Saeman J.F., 1945, Kinetics of wood saccharification hydrolysis of cellulose and decomposition of sugars in dilute acid at high temperature, Ind. Eng. Chem., 37, 43–52.

Tavares J., Sthel M., Campos L., Rocha M., Lima G., da Silva M., Vargas H., 2011, Evaluation of pollutant gases emitted by ethanol and gasoline powered vehicles, Procedia Environ. Sci., 4, 51-60.

Tovar L.P., dos Santos R.A., Wolf-Maciel M.R., Maciel-Filho R., 2013, Experimental evaluation and kinetic modeling studies on the hydrothermal and H_2SO_4-catalyzed hydrothermal pretreatments of sugarcane bagasse: focusing on pretreatment at low temperature and batch process for high-solids loading, Poster 10-31, 35th Symposium on biotechnology for fuels and chemical, April 29 - May 2, 2013, Portland, OR.